



Published in final edited form as:

Nature. 2014 May 1; 509(7498): 96–100. doi:10.1038/nature13136.

## Cystathionine $\gamma$ -lyase deficiency mediates neurodegeneration in Huntington's disease

Bindu D. Paul<sup>1</sup>, Juan I. Sbdio<sup>1</sup>, Risheng Xu<sup>1,2</sup>, M. Scott Vandiver<sup>1,2</sup>, Jiyoung Y. Cha<sup>1</sup>, Adele M. Snowman<sup>1</sup>, and Solomon H. Snyder<sup>1,2,3</sup>

<sup>1</sup>The Solomon H. Snyder Department of Neuroscience, Johns Hopkins University School of Medicine, Baltimore, Maryland 21205, USA.

<sup>2</sup>Department of Pharmacology and Molecular Sciences, Johns Hopkins University School of Medicine, Baltimore, Maryland 21205, USA.

<sup>3</sup>Department of Psychiatry, Johns Hopkins University School of Medicine, Baltimore, Maryland 21205, USA.

### Abstract

Huntington's disease is an autosomal dominant disease associated with a mutation in the gene encoding huntingtin (Htt) leading to expanded polyglutamine repeats of mutant Htt (mHtt) that elicit oxidative stress, neurotoxicity, and motor and behavioural changes<sup>1</sup>. Huntington's disease is characterized by highly selective and profound damage to the corpus striatum, which regulates motor function. Striatal selectivity of Huntington's disease may reflect the striatally selective small G protein Rhes binding to mHtt and enhancing its neurotoxicity<sup>2</sup>. Specific molecular mechanisms by which mHtt elicits neurodegeneration have been hard to determine. Here we show a major depletion of cystathionine  $\gamma$ -lyase (CSE), the biosynthetic enzyme for cysteine, in Huntington's disease tissues, which may mediate Huntington's disease pathophysiology. The defect occurs at the transcriptional level and seems to reflect influences of mHtt on specificity protein 1, a transcriptional activator for CSE. Consistent with the notion of loss of CSE as a pathogenic mechanism, supplementation with cysteine reverses abnormalities in cultures of Huntington's disease tissues and in intact mouse models of Huntington's disease, suggesting therapeutic potential.

---

CSE is a principal generator of cysteine from cystathionine<sup>3,4</sup>. Cystathionine is formed by cystathionine  $\beta$ -synthase (CBS) by condensing homocysteine and serine. CSE, CBS and 3-mercaptopyruvate sulphurtransferase use cysteine to generate the major gasotransmitter

---

© 2014 Macmillan Publishers Limited. All rights reserved

Reprints and permissions information is available at [www.nature.com/reprints](http://www.nature.com/reprints).

Correspondence and requests for materials should be addressed to S.H.S. (ssnyder@jhmi.edu).

**Online Content** Any additional Methods, Extended Data display items and Source Data are available in the online version of the paper; references unique to these sections appear only in the online paper.

**Supplementary Information** is available in the online version of the paper.

**Author Contributions** B.D.P. and S.H.S. designed the research. B.D.P., J.S., R.X., M.S.V. and J.C. conducted experiments. B.D.P., J.S. and R.X. analysed data. A.M.S. prepared plasmid constructs and provided technical assistance. B.D.P. and S.H.S. wrote the paper. The authors declare no competing financial interests.

hydrogen sulphide ( $\text{H}_2\text{S}$ )<sup>3-5</sup>. It was previously believed that CSE is restricted to peripheral tissues, whereas CBS is the principal generator of  $\text{H}_2\text{S}$  in the brain<sup>6</sup>. We detected substantial CSE in brain lysates, implying a role for the enzyme in the brain (Fig. 1a, b). In characterizing CSE-deleted mice<sup>7</sup> we noted abnormal hindlimb claspings and clenching reminiscent of mouse models of Huntington's disease, which prompted an exploration of CSE in Huntington's disease (Fig. 1c). In a striatal cell line Huntington's disease model containing 111 glutamine repeats, *STHdh*<sup>Q111/Q111</sup>(Q111), CSE protein levels were markedly decreased compared with control *STHdh*<sup>Q7/Q7</sup>(Q7) cells harbouring seven glutamine repeats (Fig. 1d, e). Brains of R6/2 mice with Huntington's disease<sup>8</sup> also showed decreased CSE levels in the striatum, cortex, hippocampus, hypothalamus and brainstem, but not in the cerebellum (Fig. 1f, g). To explore the generality of findings with R6/2 mice, we examined the Q175 mouse model of Huntington's disease<sup>9</sup>. Like the R6/2 mice, striata of the Q175 mice had diminished CSE levels (Fig. 1h, i). In brains of humans with Huntington's disease, CSE levels were profoundly reduced in the striatum (Fig. 1j-m), moderately diminished in the cerebral cortex and not altered in the cerebellum (Fig. 1l), paralleling the relative susceptibility of these brain regions to damage by Huntington's disease. Clinical staging revealed a progressive depletion of CSE with increasing severity of the disease (Fig. 1l, m). The depletion of CSE in Huntington's disease is not secondary to neurodegeneration. Thus, CSE levels were unaltered in post-mortem brain samples of patients with other neurodegenerative diseases: advanced amyotrophic lateral sclerosis, multiple sclerosis and spinocerebellar ataxia (Extended Data Fig. 1). In liver and pancreatic lysates of R6/2 mice, CSE levels were diminished to a similar extent to that in brain (Fig. 1n, o). CSE generates both cysteine and  $\text{H}_2\text{S}$  (Fig. 2a). In striatal Q111 cells we observed a diminished formation of both  $\text{H}_2\text{S}$  (Fig. 2b) and cysteine (Fig. 2c). Cysteine-free diets are lethal to CSE-deleted mice<sup>10,11</sup>, and CSE deficiency of Q111 cells was associated with cytotoxicity in the absence of cysteine (Fig. 2d). On cysteine-free medium, 80% of Q111 cells die with only modest cell loss in Q7 cells. Supplementation with  $\alpha$ -cysteine reversed the lethality (Fig. 2d), as did overexpression of CSE (Fig. 2e). Thus, the CSE depletion in Huntington's disease cells renders them hypersensitive to lethality associated with cysteine deprivation. Cysteine levels and  $\text{H}_2\text{S}$  generation were diminished in striata of R6/2 mice (Fig. 2f, g), and CSE activity was reduced in striata of Q175 mice (Fig. 2h).

How does Huntington's disease elicit CSE depletion? The loss of cytosolic CSE could reflect the translocation of CSE to insoluble aggregates, which occurs in Huntington's disease<sup>12,13</sup>. However, in Q111 cells CSE was depleted to similar extents in supernatant and particulate fractions (Fig. 3a). CSE is probably not depleted by proteasomal enzymes, because the proteasomal inhibitor MG132 failed to elevate the very low levels of CSE in Q111 cells (Fig. 3b).

Might depletion of CSE occur at a transcriptional level? Consistent with this possibility, analysis by PCR with reverse transcription (RT-PCR) revealed a marked decrease in mRNA levels for CSE in Q111 cells (Fig. 3c, d). Moreover, reporter gene assays revealed substantially reduced CSE promoter activity in Q111 cells (Fig. 3e). Thus, CSE transcription in Huntington's disease is evidently impaired at the level of transcriptional regulation. mHtt can elicit toxicity by disrupting transcriptional processes<sup>14,15</sup>: it has been reported<sup>16</sup> that

mHtt binds to and inhibits specificity protein 1 (Sp1), a known transcription factor for CSE<sup>17,18</sup>. Overexpression of both Sp1 and its co-activator transcription initiation factor TFIID subunit 4 (TAF4) rescued the diminished messenger RNA and protein levels of CSE in Q111 cells (Fig. 3f–h) and improved growth in cysteine-free growth medium (Fig. 3i). Thus, CSE depletion in Huntington's disease seems to reflect an inhibition of Sp1 by mHtt, leading to decreased CSE transcription.

Huntington's disease is associated with heightened oxidative stress and mitochondrial dysfunction<sup>19</sup>, and CSE has a function in mitochondrial homeostasis<sup>20</sup>. To assess whether CSE depletion elicits oxidative and mitochondrial stress, we treated wild-type and *Cse*<sup>-/-</sup> mice with 3-nitropropionic acid, a mitochondrial toxin that inhibits the complex II enzyme succinate dehydrogenase<sup>21</sup>. Treatment with 3-nitropropionic acid causes mitochondrial dysfunction and oxidative stress, thereby damaging striatal tissue and mimicking Huntington's disease<sup>22</sup>. *Cse*<sup>-/-</sup> mice were highly susceptible to 3-nitropropionic acid, showing elevated levels of protein carbonylation and nitration in the striatum and cortex (Extended Data Fig. 2). In addition, striatal Q111 cells showed greater susceptibility to hydrogen peroxide stress, and overexpressing CSE increased their resistance to H<sub>2</sub>O<sub>2</sub> (Fig. 4a). If the pathophysiology of Huntington's disease reflects, at least in part, CSE depletion, we might predict neurobehavioural aberrations in CSE deleted mice. *Cse*<sup>-/-</sup> mice showed impaired rotarod performance (Fig. 4b). *Cse*<sup>+/-</sup> heterozygous mice also showed impaired motor functions, although not as severe as in the homozygous *Cse*<sup>-/-</sup> mice (Fig. 4b).

By what molecular mechanisms might CSE exert cytoprotection? CSE is a major generator of cysteine, which is a building block for proteins and the antioxidant glutathione. In addition, cysteine is a precursor of H<sub>2</sub>S, which signals by attaching a thiol group to target proteins, a process termed sulphhydration; this process typically activates enzymes, some of which are involved in cytoprotection<sup>3,23,24</sup>. For instance, H<sub>2</sub>S sulphhydrates parkin to stimulate its catalytic activity, which provides striatal neuroprotection relevant to Parkinson's disease<sup>25</sup>. H<sub>2</sub>S also sulphhydrates Keap1 (ref. 26), a repressor of the transcription factor Nrf2, which regulates several enzymes of the antioxidant defence pathway. In addition, H<sub>2</sub>S influences several cytoprotective pathways<sup>27</sup>. It is unclear whether the pathophysiological influences of CSE depletion in Huntington's disease reflect its role in generating cysteine or H<sub>2</sub>S. It is conceivable that treatment with H<sub>2</sub>S donors will be beneficial in treating Huntington's disease.

The ability of CSE and cysteine to reverse oxidative stress and lethality in Huntington's disease cells suggests that cysteine supplementation might be beneficial in treating Huntington's disease. Cysteine deficiency has been implicated in oxidative stress and ageing<sup>28</sup>. Cystamine, the decarboxylated derivative of cystine (the disulphide of cysteine) confers neuroprotection in mouse models of Huntington's disease and increases cysteine levels in the brain<sup>29</sup>. Treating R6/2 mice with *N*-acetylcysteine (a stable precursor of cysteine) in their drinking water along with a cysteine-enriched diet delayed the onset of motor abnormalities such as hindlimb clasping (Fig. 4c and Supplementary Videos 1–3), rotarod performance (Fig. 4d) and grip strength (Fig. 4e). Decreases in brain weight and striatal were partly reversed by treatment with cysteine (Fig. 4f–h), and survival was enhanced (Fig. 4i).

Although many molecular targets of mHtt have been described, specific mechanisms that underlie Huntington's disease neurotoxicity have been hard to determine. It has been reported<sup>16</sup> that binding of mHtt to the transcriptional activator Sp1 mediates neurotoxicity by diminishing Sp1 activity. We propose that inhibition by mHtt of Sp1's transcriptional activation of CSE accounts for CSE depletion in Huntington's disease and associated neurological deficits. This CSE model of Huntington's disease is supported by the therapeutic effects of cysteine and *N*-acetylcysteine in mice with Huntington's disease. Our findings imply that *N*-acetylcysteine supplementation may be beneficial in treating diseases involving impaired reverse transsulphuration and oxidative stress.

## METHODS

### Plasmids, cell lines and chemicals

The plasmids encoding Sp1 and TAF4 were gifts from D. Krainc (Massachusetts General Hospital, Boston, Massachusetts). The plasmid encoding CSE was described previously. The striatal cell lines *STHdh*<sup>Q7/Q7</sup>, expressing wild-type huntingtin, and *STHdh*<sup>Q111/Q111</sup>, expressing mutant huntingtin with 111 glutamine repeats (referred to as Q7 and Q111 cells, respectively), were from M. MacDonald (Department of Neurology, Massachusetts General Hospital, Boston). Unless otherwise mentioned, all chemicals were from Sigma. Lipofectamine 2000 (Invitrogen) was used for all transfection studies.

### Western blotting

Cells were lysed on ice for 15 min in buffer containing 50 mM Tris-HCl pH 8.0, 150 mM NaCl, 1% Triton X-100 and protease inhibitors, followed by centrifugation and recovery of the supernatant. The pellet fraction was resuspended in 2% SDS lysis buffer followed by sonication. Protein concentrations were estimated with the bicinchoninic acid assay (Thermo Scientific). Anti-CSE antibodies were described previously<sup>7</sup>. The human post-mortem samples were obtained from J. Troncoso (Brain Resource Center, Johns Hopkins University).

### RNA isolation and RT-PCR

Total RNA was isolated from cells and tissues using Trizol reagent followed by the RNEasy Lipid Tissue kit (Qiagen). Conventional RT-PCR was performed with the Superscript One-Step RT-PCR kit (Invitrogen). Real-time quantitative PCR was performed with the TaqMan RNA-to-Ct 1-Step Kit and the Step One Plus instrument (Life Technologies).

### H<sub>2</sub>S production assay

The H<sub>2</sub>S production assay was as described previously<sup>7,20</sup>.

### Cysteine production assay

Cysteine formed by CSE was quantified as described previously<sup>7</sup>. Ninhydrin reagent was prepared by dissolving 250 mg of ninhydrin in 6 ml of glacial acetic acid and 4 ml of 12 M HCl. Samples (200 µl) were mixed with 60 µl of 6% perchloric acid, and precipitated protein was removed by centrifugation. Next, 200 µl of the supernatant was mixed with 200 µl of

glacial acetic acid and ninhydrin, then boiled for 10 min, cooled on ice and mixed with 95% ethanol to a final volume of 1 ml. The absorbance was measured at 560 nm.

### Animals and treatments

Animals were housed on a 12 h light–dark schedule and received food and water *ad libitum*. The R6/2 (B6CBA-Tg(HDexon1)62Gpb/1J) transgenic mice were from the Jackson Laboratory. The *Cse*<sup>-/-</sup> mice were described previously<sup>7</sup>. All animals were treated in accordance with the recommendations of the National Institutes of Health and approved by the Johns Hopkins University Committee on Animal Care.

### Cysteine treatment of R6/2 mice

All wild-type and R6/2 mice offspring derived from mice hemizygous for Tg(HDexon1)62Gpb (ovary transplant) were placed either on an AIN93 mineral diet with 0.3% cystine or on an AIN93 diet containing 0.8% cystine (Teklad Lab Animal Diets; Harlan Laboratories) starting at 4 weeks of age. In addition, the mice on diets containing high cysteine were also given 20 mM *N*-acetylcysteine in the drinking water. Survival and motor phenotypes of the mice were recorded.

### Motor tests

The motor functions of the mice were tested with the hindlimb clasping function. Mice were suspended by their tail and the time taken to clasp was recorded. The accelerating rotarod was performed on a Rotamex V (Columbus Instruments) with speeds that varied from 4 to 40 r.p.m. for a maximum of 5 min with an acceleration interval of 30 s. Seven-week-old male R6/2 mice were used for the rotarod assay; 8-month-old male *Cse*<sup>-/-</sup> mice were used for the assay. The grip test was performed on 11-week-old male mice by placing the mouse over the baseplate by the tail such that its forelimbs grasped the metal grid. The tail was gently pulled backward until the grip was released. The force required to release the grip was recorded by the grip strength meter.

### Statistical analyses

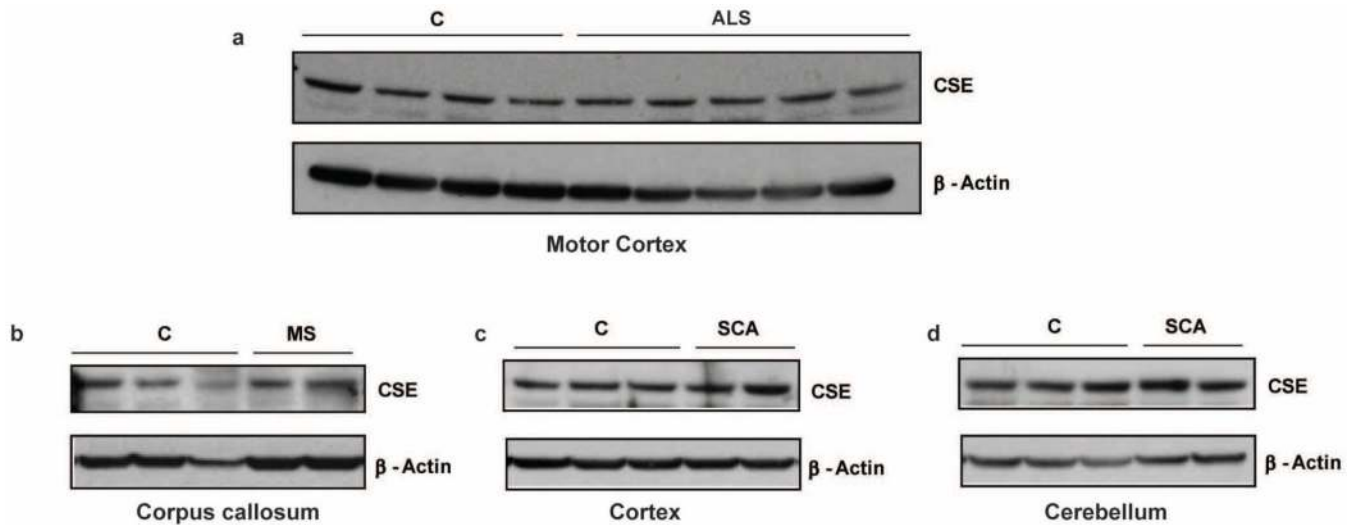
Results are presented as means  $\pm$  s.e.m. for at least three independent experiments. The sample sizes used were based on the magnitude of changes and consistency expected. Statistical significance was reported as appropriate. In experiments involving animals, no exclusions were done. Sample sizes were chosen on the basis of the magnitude of changes expected. No randomization methods were used. In behavioural analyses, the experimenter conducting the test was blinded to the genotype or treatment of the animals under study. *P* values were calculated with Student's *t*-test.

### Histology and quantification of relative striatal volume

Male mice at 12 weeks of age were perfused transcardially with 4% paraformaldehyde (PFA) in PBS and brains were stored overnight in 4% PFA in PBS. Next, brains were cryoprotected in 30% sucrose in PBS and sectioned with a freezing microtome at a section thickness of 30  $\mu$ m. Sections were mounted on glass slides and allowed to dry at 25 °C for 24 h and then stained with Nissl stain. Striatal volumes were calculated using Cavalieri's

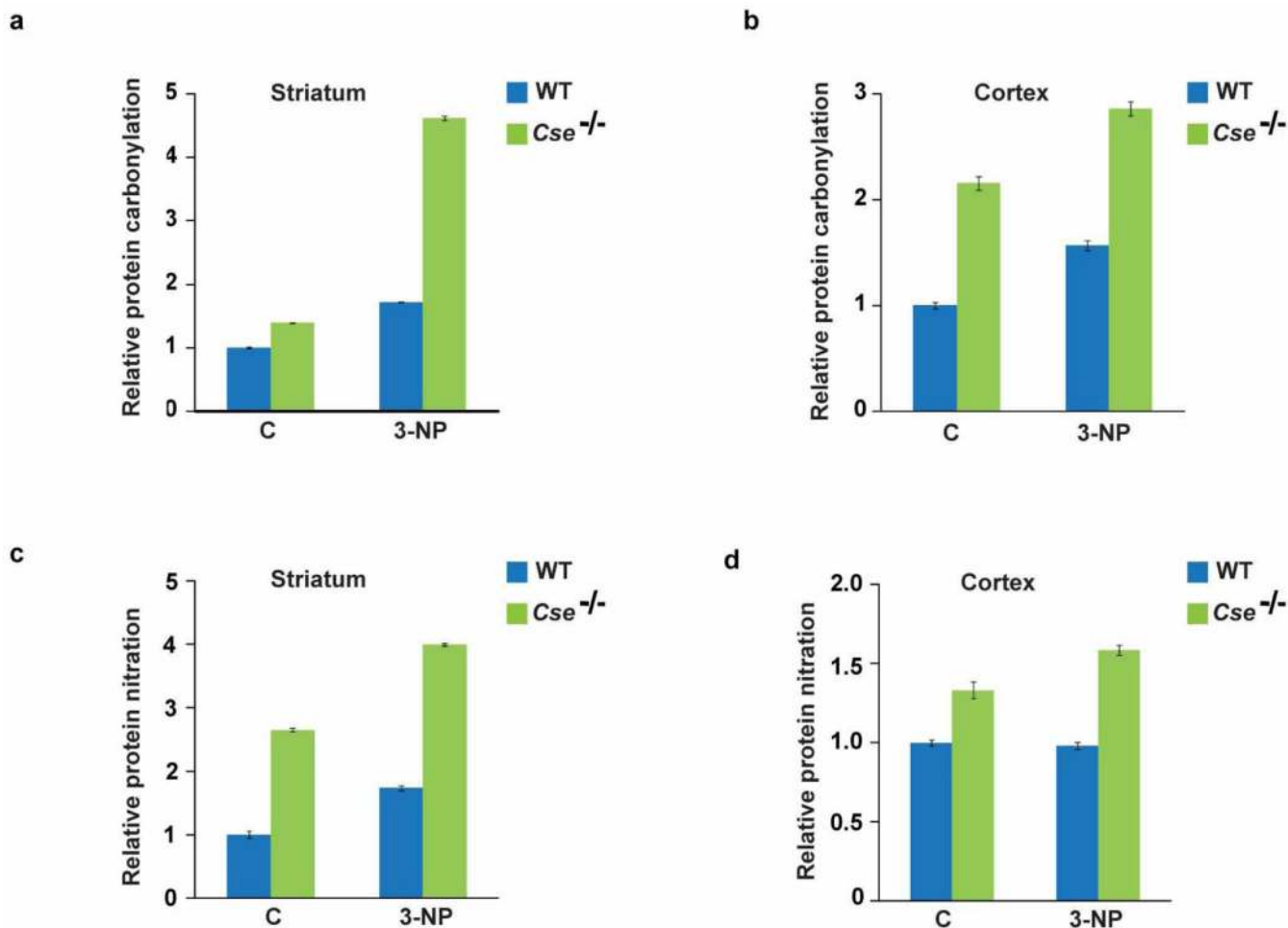
principle<sup>30</sup> (volume =  $s_1d_1 + s_2d_2 + \dots + s_nd_n$ , where  $s$  is surface area and  $d$  is the distance between two sections).

## Extended Data



### Extended Data Figure 1. CSE expression is not altered in the brain in amyotrophic lateral sclerosis, multiple sclerosis and spinocerebellar ataxia

**a**, Western blots show that CSE expression in the motor cortex of samples from controls and patients with amyotrophic lateral sclerosis (ALS) showing substantial neurodegeneration in the motor cortex are similar. Extracts were prepared from the motor cortex and analysed for CSE expression using anti-CSE antibodies and  $\beta$ -actin as a loading control. **b**, Expression of CSE is not altered in the corpus callosum of patients with multiple sclerosis (MS), where multiple lesions, demyelination and decrease in oligodendrocytes was observed in the corpus callosum of the brain. **c**, **d**, Levels of CSE do not change in the cerebral cortex (**c**) or cerebellum (**d**) of patients with spinocerebellar ataxia (SCA). Neuropathological analysis of the brains of these patients revealed severe neuronal loss and gliosis in the cerebellum.



#### Extended Data Figure 2. *Cse*<sup>-/-</sup> mice are more vulnerable to stress induced by 3-nitropropionic acid

Wild-type and *Cse*<sup>-/-</sup> male mice at 8 months of age were injected with a single dose of 3-nitropropionic acid (3-NP) (100 mg kg<sup>-1</sup>), and lysates were prepared 24 h later from the striatum and cortex and analysed for oxidative stress. **a, b**, Striata (**a**) and cortex (**b**) of *Cse*<sup>-/-</sup> mice show elevated protein oxidation as measured by protein carbonylation, which is more pronounced in the striatum.  $n = 3$  (means  $\pm$  s.e.m.). **c, d**, *Cse*<sup>-/-</sup> mice also show augmented levels of protein nitration in the striatum (**c**) and cortex (**d**) in comparison with wild-type mice. Note the increased basal level of protein oxidation in the *Cse*<sup>-/-</sup> mice.

## Supplementary Material

Refer to Web version on PubMed Central for supplementary material.

## Acknowledgements

We thank J. C. Troncoso and O. Pletnikova for providing the human post-mortem tissue samples; D. Krainc for the constructs CMV-SP1 and TAF4; M. MacDonald for the striatal Q7 and Q111 cell lines; and the Cure Huntington's Disease Initiative (CHDI) for the Q175 mice tissues. This work was supported by United States Public Health Service Grant MH 18501 to S.H.S. and by the CHDI. M.S.V. and R.X. are supported by the National Institutes of Health Medical Scientist Training Program Award.



## References

1. Huntington's Disease Collaborative Research Group. A novel gene containing a trinucleotide repeat that is expanded and unstable on Huntington's disease chromosomes. *Cell*. 1993; 72:971–983. [PubMed: 8458085]
2. Subramaniam S, Snyder SH. Huntington's disease is a disorder of the corpus striatum: focus on Rhes (Ras homologue enriched in the striatum). *Neuropharmacology*. 2011; 60:1187–1192. [PubMed: 21044641]
3. Paul BD, Snyder SH. H<sub>2</sub>S signalling through protein sulphydration and beyond. *Nature Rev. Mol. Cell Biol.* 2012; 13:499–507. [PubMed: 22781905]
4. Wang R. Physiological implications of hydrogen sulfide: a whiff exploration that blossomed. *Physiol. Rev.* 2012; 92:791–896. [PubMed: 22535897]
5. Kimura H. Hydrogen sulfide: its production, release and functions. *Amino Acids*. 2011; 41:113–121. [PubMed: 20191298]
6. Morikawa T, et al. Hypoxic regulation of the cerebral microcirculation is mediated by a carbon monoxide-sensitive hydrogen sulfide pathway. *Proc. Natl Acad. Sci. USA*. 2012; 109:1293–1298. [PubMed: 22232681]
7. Yang G, et al. H<sub>2</sub>S as a physiologic vasorelaxant: hypertension in mice with deletion of cystathionine  $\gamma$ -lyase. *Science*. 2008; 322:587–590. [PubMed: 18948540]
8. Mangiarini L, et al. Exon 1 of the HD gene with an expanded CAG repeat is sufficient to cause a progressive neurological phenotype in transgenic mice. *Cell*. 1996; 87:493–506. [PubMed: 8898202]
9. Menalled LB, et al. Comprehensive behavioral and molecular characterization of a new knock-in mouse model of Huntington's disease: zQ175. *PLoS ONE*. 2012; 7:e49838. [PubMed: 23284626]
10. Ishii I, et al. Cystathionine  $\gamma$ -lyase-deficient mice require dietary cysteine to protect against acute lethal myopathy and oxidative injury. *J. Biol. Chem.* 2010; 285:26358–26368. [PubMed: 20566639]
11. Mani S, Yang G, Wang R. A critical life-supporting role for cystathionine  $\gamma$ -lyase in the absence of dietary cysteine supply. *Free Radic. Biol. Med.* 2011; 50:1280–1287. [PubMed: 21310231]
12. DiFiglia M, et al. Aggregation of huntingtin in neuronal intranuclear inclusions and dystrophic neurites in brain. *Science*. 1997; 277:1990–1993. [PubMed: 9302293]
13. Davies SW, et al. Formation of neuronal intranuclear inclusions underlies the neurological dysfunction in mice transgenic for the HD mutation. *Cell*. 1997; 90:537–548. [PubMed: 9267033]
14. Sugars KL, Rubinsztein DC. Transcriptional abnormalities in Huntington disease. *Trends Genet.* 2003; 19:233–238. [PubMed: 12711212]
15. Zhai W, Jeong H, Cui L, Krainc D, Tjian R. *In vitro* analysis of huntingtin-mediated transcriptional repression reveals multiple transcription factor targets. *Cell*. 2005; 123:1241–1253. [PubMed: 16377565]
16. Dunah AW, et al. Sp1 and TAFII130 transcriptional activity is disrupted in early Huntington's disease. *Science*. 2002; 296:2238–2243. [PubMed: 11988536]
17. Ishii I, et al. Murine cystathionine  $\gamma$ -lyase: complete cDNA and genomic sequences, promoter activity, tissue distribution and developmental expression. *Biochem. J.* 2004; 381:113–123. [PubMed: 15038791]
18. Yang G, Pei Y, Teng H, Cao Q, Wang R. Specificity protein-1 as a critical regulator of human cystathionine  $\gamma$ -lyase in smooth muscle cells. *J. Biol. Chem.* 2011; 286:26450–26460. [PubMed: 21659522]
19. Lin MT, Beal MF. Mitochondrial dysfunction and oxidative stress in neurodegenerative diseases. *Nature*. 2006; 443:787–795. [PubMed: 17051205]
20. Fu M, et al. Hydrogen sulfide (H<sub>2</sub>S) metabolism in mitochondria and its regulatory role in energy production. *Proc. Natl Acad. Sci. USA*. 2012; 109:2943–2948. [PubMed: 22323590]
21. Alston TA, Mela L, Bright HJ. 3-Nitropropionate, the toxic substance of *Indigofera*, is a suicide inactivator of succinate dehydrogenase. *Proc. Natl Acad. Sci. USA*. 1977; 74:3767–3771. [PubMed: 269430]



22. Brouillet E, Jacquard C, Bizat N, Blum D. 3-Nitropropionic acid: a mitochondrial toxin to uncover physiopathological mechanisms underlying striatal degeneration in Huntington's disease. *J. Neurochem.* 2005; 95:1521–1540. [PubMed: 16300642]
23. Mustafa AK, et al. H<sub>2</sub>S signals through protein S-sulfhydration. *Sci. Signal.* 2009; 2:ra72. [PubMed: 19903941]
24. Sen N, et al. Hydrogen sulfide-linked sulfhydration of NF-κB mediates its antiapoptotic actions. *Mol. Cell.* 2012; 45:13–24. [PubMed: 22244329]
25. Vandiver MS, et al. Sulfhydration mediates neuroprotective actions of parkin. *Nature. Commun.* 2013; 4:1626. [PubMed: 23535647]
26. Yang G, et al. Hydrogen sulfide protects against cellular senescence via S-sulfhydration of Keap1 and activation of Nrf2. *Antioxid. Redox Signal.* 2013; 18:1906–1919. [PubMed: 23176571]
27. Szabo C. Hydrogen sulphide and its therapeutic potential. *Nature Rev. Drug Discov.* 2007; 6:917–935. [PubMed: 17948022]
28. Droge W. Oxidative stress and ageing: is ageing a cysteine deficiency syndrome? *Phil. Trans. R. Soc. Lond. B.* 2005; 360:2355–2372. [PubMed: 16321806]
29. Fox JH, et al. Cystamine increases l-cysteine levels in Huntington's disease transgenic mouse brain and in a PC12 model of polyglutamine aggregation. *J. Neurochem.* 2004; 91:413–422. [PubMed: 15447674]
30. Cyr M, Caron MG, Johnson GA, Laakso A. Magnetic resonance imaging at microscopic resolution reveals subtle morphological changes in a mouse model of dopaminergic hyperfunction. *Neuroimage.* 2005; 26:83–90. [PubMed: 15862208]

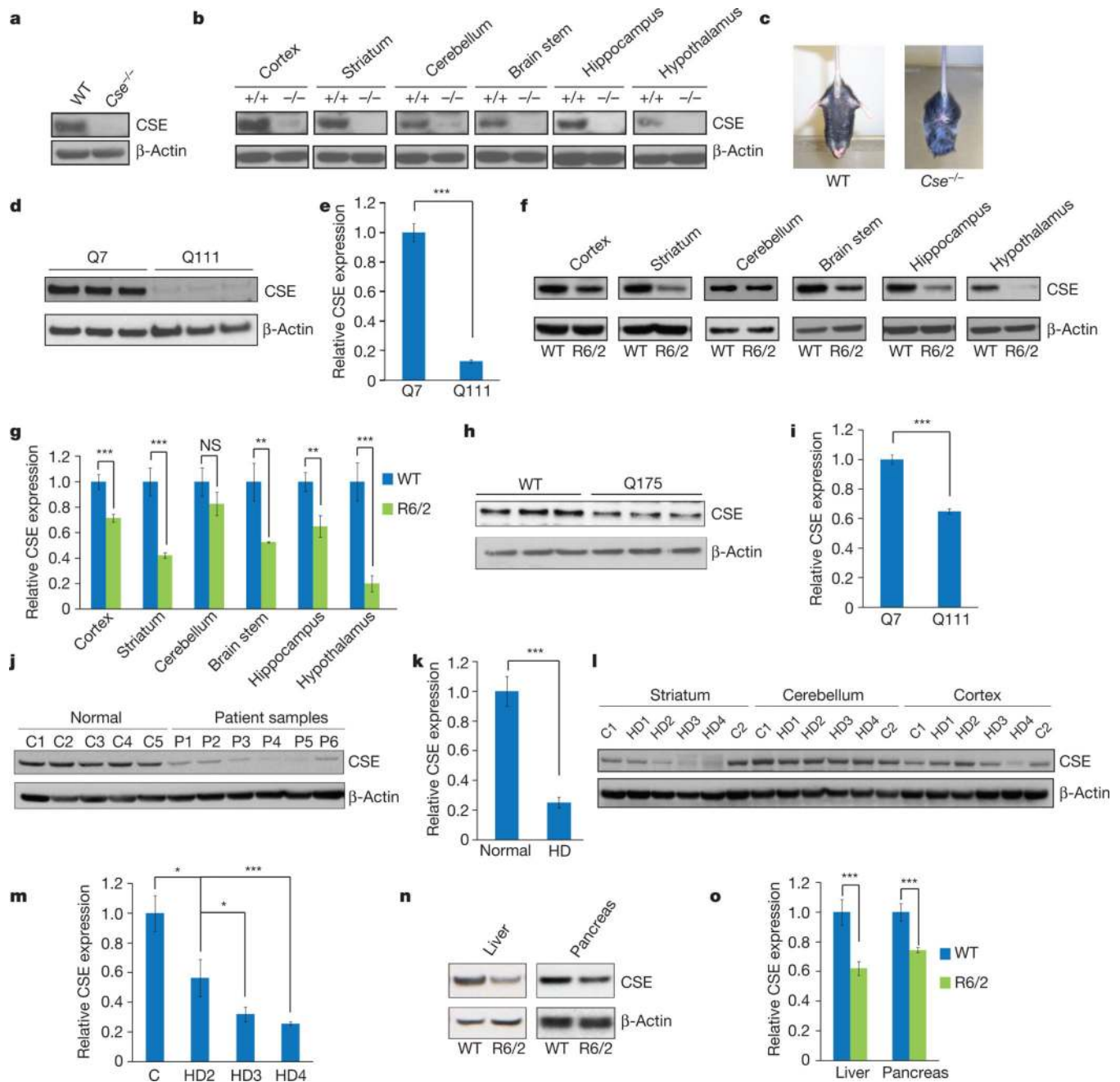


**Figure 1. CSE is expressed in the brain and is depleted in Huntington's disease**

**a**, CSE expression is detectable in whole-brain lysates. WT, wild type. **b**, CSE is expressed in different regions of the brain. **c**, *Cse*<sup>-/-</sup> mice show a limb-clasping phenotype. **d**, Striatal *STHdh*<sup>Q111/Q111</sup> have decreased expression of CSE. **e**, Quantification of **d**. *n* = 3 (means ± s.e.m.); \*\*\**P* < 0.001. **f**, Expression of CSE is decreased significantly in all brain regions of 13-week-old R6/2 mice analysed except in the cerebellum. **g**, Relative quantification of **f**. *n* = 6 (means ± s.e.m.) for cortex, striatum and cerebellum; *n* = 3 (means ± s.e.m.) for other regions; \*\*\**P* < 0.001; \*\**P* < 0.01; NS, not significant. **h**, Expression of CSE is decreased in striata of Q175 mice. **i**, Quantification of **h**. *n* = 3 (means ± s.e.m.); \*\*\**P* < 0.001. **j**, Post-

mortem striatal brain samples (P1–P6) from patients with Huntington’s disease show a decrease in CSE expression. **k**, Relative quantification of **j**.  $n = 5$  (means  $\pm$  s.e.m.) for controls;  $n = 6$  (means  $\pm$  s.e.m.) for samples from patients with Huntington’s disease (HD);  $***P < 0.001$ . **l**, CSE depletion is increased with the severity of the disease. C1 and C2 are controls; HD1–HD4 are samples from patients with Huntington’s disease. **m**, Relative quantification of HD grades.  $n = 3$  (means  $\pm$  s.e.m.) for HD2;  $n = 4$  (means  $\pm$  s.e.m.) for normal, HD3 and HD4;  $*P < 0.05$  (control versus HD2 and HD2 versus HD3);  $***P < 0.001$  (control versus HD4). **n**, CSE expression is decreased in the liver and pancreas. **o**, Relative quantification of **n**.  $n = 3$  (means  $\pm$  s.e.m.);  $***P < 0.001$ .

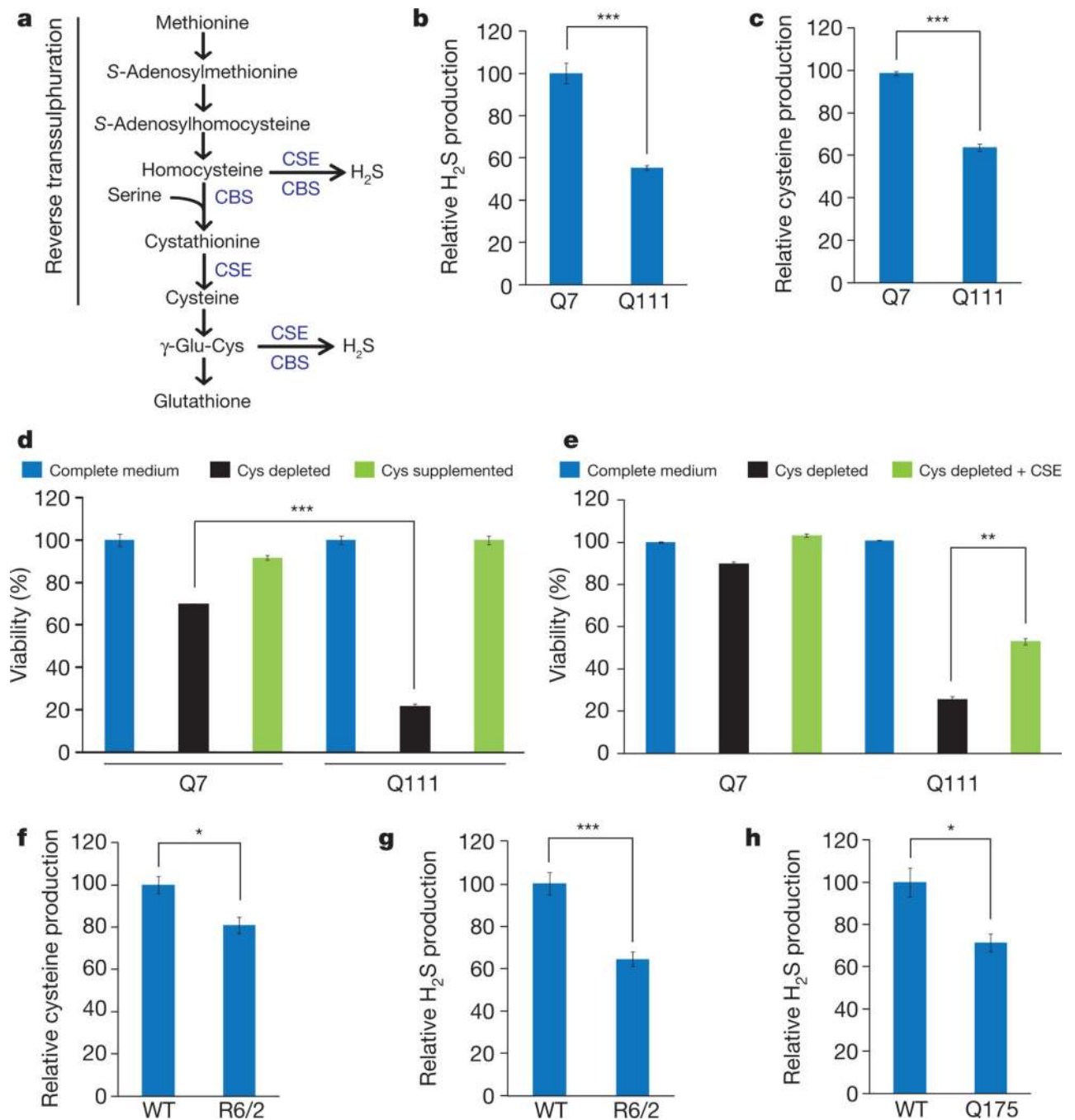


**Figure 2. Decreased CSE activity and growth in striatal Q111 cells**

**a**, The reverse transsulfuration pathway leading to the production of cysteine from methionine. CSE produces cysteine from cystathionine generated by CBS. Cysteine and homocysteine are substrates for the production of H<sub>2</sub>S. **b**, Decreased H<sub>2</sub>S production in Q111 cells in comparison with Q7 cells.  $n = 3$  (means  $\pm$  s.e.m.); \*\*\* $P < 0.001$ . **c**, Decreased cysteine synthesis in Q111 cells.  $n = 3$  (means  $\pm$  s.e.m.); \*\*\* $P < 0.001$ . **d**, Impaired growth of Q111 cells in cysteine-free medium as monitored by the 3-(4,5-dimethylthiazol-2-yl)-2,5-diphenyl-2H-tetrazolium bromide (MTT) assay. Q111 cells underwent cell death, which was

rescued by supplementation with L-cysteine.  $n = 3$  (means  $\pm$  s.e.m.);  $***P < 0.001$ . **e**, Growth retardation of Q111 cells in cysteine-free medium is rescued by the transfection of CSE construct as assessed by the MTT assay.  $**P < 0.01$ . **f**, Decreased cysteine levels in striata of R6/2 mice.  $n = 3$  (means  $\pm$  s.e.m.);  $*P < 0.05$ . **g**, Decreased synthesis of H<sub>2</sub>S in striata of R6/2 mice.  $n = 3$  (means  $\pm$  s.e.m.);  $***P < 0.001$ . **h**, Decreased synthesis of H<sub>2</sub>S in striata of Q175 mice.  $n = 3$  (means  $\pm$  s.e.m.);  $*P < 0.05$ .

Author Manuscript

Author Manuscript

Author Manuscript

Author Manuscript

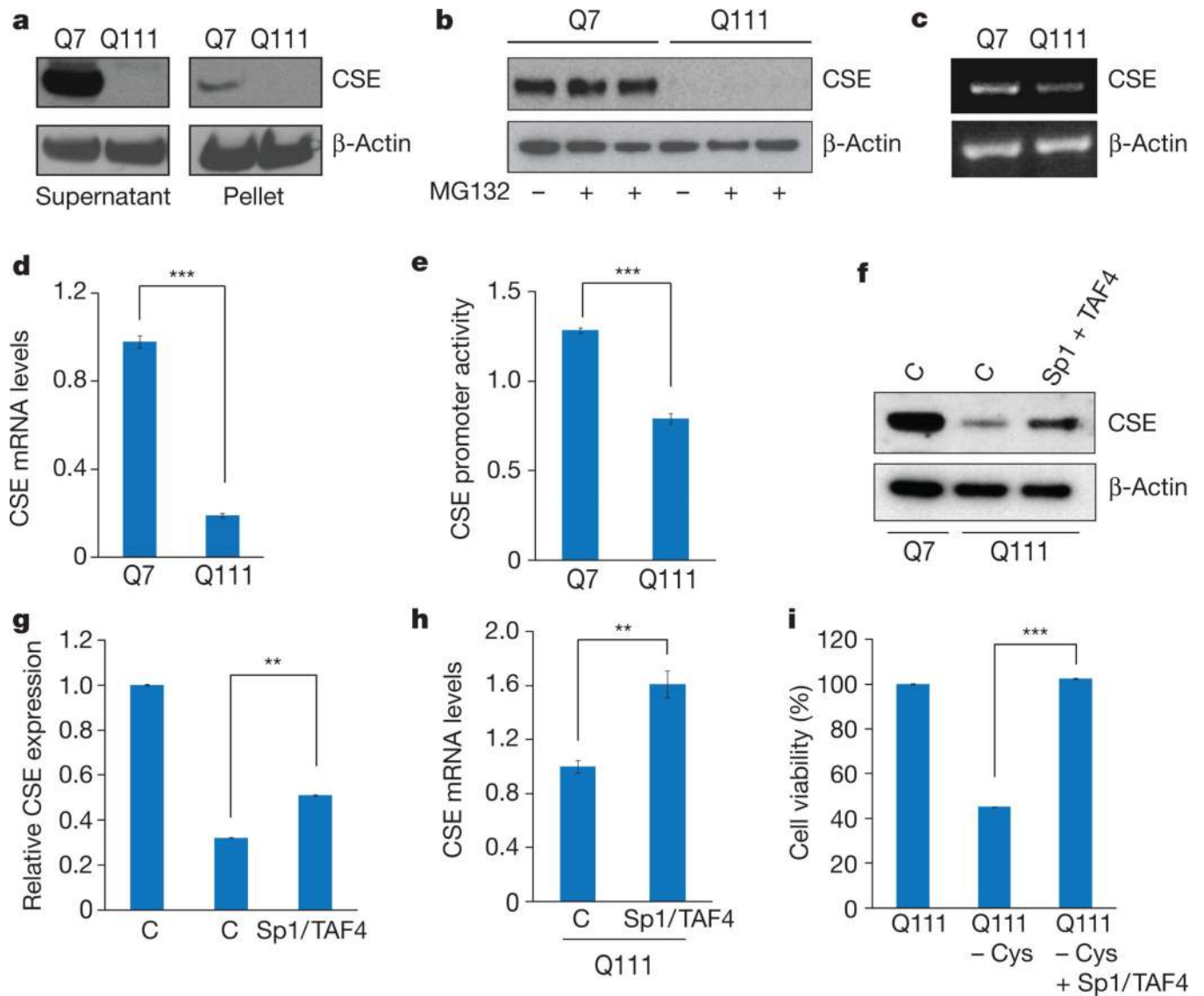


**Figure 3. CSE is depleted at the transcriptional level in Huntington's disease**

**a**, CSE is not sequestered in the insoluble pellet fraction by mutant huntingtin. **b**, CSE is not differentially degraded in Q7 and Q111 cells after treatment with the proteasome inhibitor MG132. **c**, CSE mRNA is decreased in Q111 cells, as revealed by RT-PCR using  $\beta$ -actin as the internal control. **d**, Reduction of CSE expression in Q111 cells verified by real-time quantitative PCR.  $n = 3$  (means  $\pm$  s.e.m.);  $***P < 0.001$ . **e**, CSE promoter activity is repressed in Q111 cells as revealed by luciferase assays using a CSE-luc reporter construct and an endogenous internal control.  $n = 4$  (means  $\pm$  s.e.m.);  $***P < 0.001$ . **f**, Overexpression of the transcription factor Sp1 and its co-activator TAF4 rescues CSE expression. Empty vector controls are denoted by C. **g**, Relative quantification of **f**.  $n = 3$  (means  $\pm$  s.e.m.);  $**P < 0.01$ . **h**, Overexpression of Sp1 and TAF4 elevates CSE transcript levels as revealed by quantitative PCR.  $n = 3$  (means  $\pm$  s.e.m.);  $**P < 0.01$ . **i**, Overexpression of Sp1/TAF4 rescues lethality of Q111 cells in cysteine-free media as measured by the MTT assay.  $n = 3$  (means  $\pm$  s.e.m.);  $***P < 0.001$ .



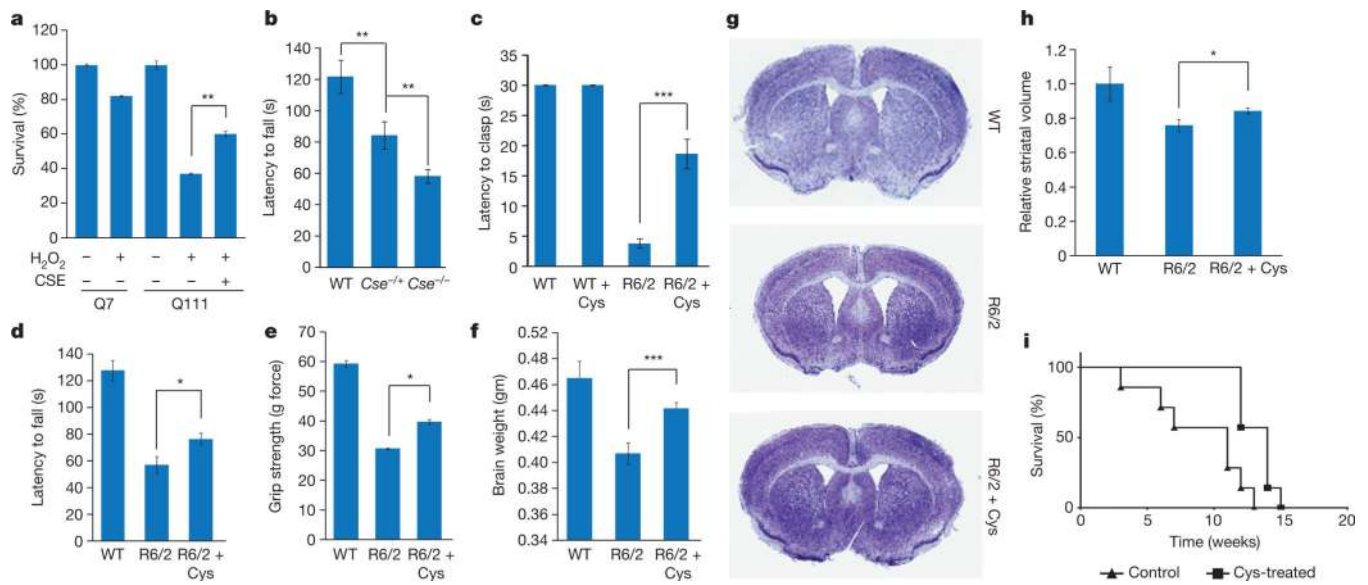


**Figure 4. CSE protects against oxidative stress, and cysteine supplementation delays neurodegeneration**

**a**, Striatal Q111 cells are more vulnerable to oxidative stress induced by 0.1 mM  $H_2O_2$  as monitored by MTT assays, effects that are rescued by CSE overexpression.  $n = 3$  (means  $\pm$  s.e.m.);  $**P < 0.01$ . **b**,  $Cse^{-/-}$  mice have impaired motor function. WT,  $Cse^{-/-}$  homozygous and  $Cse^{+/-}$  heterozygous mice were placed on an accelerating rotarod, and latency to fall was recorded. Both the  $Cse^{-/-}$  homozygous and  $Cse^{+/-}$  heterozygous mice were impaired in their motor functions; the homozygous knockout mice showed the greatest deficits.  $n = 5$  (means  $\pm$  s.e.m.) for WT,  $n = 4$  (means  $\pm$  s.e.m.) for  $Cse^{+/-}$  heterozygous and  $n = 11$  for  $Cse^{-/-}$  homozygous;  $***P < 0.001$  (WT versus  $Cse^{-/-}$ );  $**P < 0.01$  (WT versus  $Cse^{+/-}$  and  $Cse^{+/-}$  versus  $Cse^{-/-}$ ). **c**, Cysteine supplementation delays motor symptoms in R6/2 mice. Mice were placed on regular diet or a cysteine-supplemented diet along with 20 mM *N*-acetylcysteine in the drinking water, and clasp phenotype was monitored.  $n = 8$  (means  $\pm$  s.e.m.);  $***P < 0.001$ . See also Supplementary Videos 1–3. **d**, Cysteine supplementation improves performance on an accelerating rotarod in R6/2 mice.  $n = 8$  (means  $\pm$  s.e.m.) for WT;  $n = 6$  (means  $\pm$  s.e.m.) for R6/2;  $n = 7$  (means  $\pm$  s.e.m.) for R6/2 + cysteine;  $*P < 0.05$ . **e**, Grip strength is improved in R6/2 mice placed on a cysteine-supplemented diet.  $*P < 0.05$ . **f**, Decrease in brain masses of R6/2 mice is ameliorated by cysteine treatment. **g**, Striatal atrophy is decreased in R6/2 mice treated with cysteine as assessed by Nissl staining of coronal sections of the brain. **h**, Striatal volume of R6/2 mice on a cysteine supplemented diet is larger than in the untreated R6/2 mice.  $n = 3$  (means  $\pm$  s.e.m.) for WT,  $n = 4$  (means  $\pm$  s.e.m.) for untreated R6/2 mice and R6/2 mice treated with cysteine.  $*P < 0.05$ . **i**, Cysteine supplementation prolongs survival in R6/2 mice (Kaplan–Meier analysis). R6/2 mice ( $n = 7$  per group) were treated as in **f**, and survival in weeks was monitored. Statistical analysis was conducted with the log-rank (Mantel–Cox) test;  $P = 0.004$ .